



International Journal of Multidisciplinary Research and Growth Evaluation



International Journal of Multidisciplinary Research and Growth Evaluation

ISSN: 2582-7138

Received: 04-05-2021; Accepted: 20-05-2021

www.allmultidisciplinaryjournal.com

Volume 2; Issue 3; May-June 2021; Page No. 378-384

Decline in stiffness of bridge structures due to resonance regions in power spectrum density

Thanh Q Nguyen¹

¹ Faculty of Engineering and Technology, Thu Dau Mot University, Binh Duong Province, Vietnam

¹ Thu Dau Mot University, Binh Duong Province, Vietnam

Corresponding Author: **Thanh Q Nguyen**

Abstract

This article proposes a method of evaluating the mechanical responses of damage detection in spans. This approach can monitor the stiffness degradation of structure spans over time. These monitoring processes should be conducted at different measuring points on spans, on different spans in the same or different measuring periods. The obtained results show that

changes in acreage in the resonance regions of the power spectrum density offer many positive preliminary outcomes for the evaluation of the quality of projects during their operational periods. This study also shows that changes in acreage in resonance regions enable the identification of dangerous points on the different spans of a bridge.

Keywords: damage detection, monitoring, resonance regions, dangerous spans, bridge

Introduction

Civil infrastructure, including bridges, plays an important role in social activities. Damage in bridges causes not only traffic stagnation and economic losses but also loss of human lives. Therefore, damage identification and condition assessment of bridges are a main task of infrastructure management communities to ensure safety in operation. With the damage identification method, many early damage detection techniques consist of experimental approaches, such as visual tests; tap tests; and acoustic or ultrasonic, stress wave, magnetic field, radiography, eddy-current and thermal field methods. These non-destructive damage detection methods are known as “local” damage detection methods or visual inspection. A disadvantage of these methods is that they require prior knowledge of the possible damage sites; hence, these methods can only be applied to accessible portions of structures^[1, 2, 3]. Moreover, these methods are generally costly, time consuming, and ineffective for large, complex structural systems. Visual inspection, which depends highly on the decisions and opinions of inspectors, can lead to large variations and subjectivity in results. Furthermore, since one can only assess the outward appearance of a structure, major internal damage can be overlooked for years^[4, 5, 6]. However, local methods are still widely used today for different infrastructures.

Change of structure is the evaluation of the load rating; it is also known as load-carrying capacity assessment by triennial inspection. This process determines the relationship between the live or overweight loads and structural responses of a bridge. These responses are usually strain, deflection, impact factor, and fundamental frequency (which only determines the first fundamental frequency). Except fundamental frequency determined from damping vibration, responses are only determined via the steady-state response of a bridge. Since the strain and deflection of a bridge is measured with known loads, this procedure offers confidence to management communities. However, this procedure is costly and requires bridge closure, which causes traffic stagnation; thus, inspection is performed triennially to perennially only. This approach has limited ability to detect all possible damages in a bridge, and it may overlook damage that grows during the two years interval. If only damage identification and condition assessment of bridges will be mandated by the National Bridge Inspection Program, the response information of bridges can be missed. In August 2007, The I-35W Mississippi River Bridge suddenly collapsed, killing 13 people and injuring 144 more, although the bridge was being inspected annually since 1993^[7]. The bridge was 40 years old and had been subjected to increased traffic and environmental loads over its lifetime, which caused deterioration and ultimately the failure of some under-designed components. In the recent 20 years, cable-stayed bridges with large lengths have been built around the world^[8, 9, 10]. They often connect a mainland with an island to a continent, hence becoming heavily influenced by environmental elements, including^[11, 12] wind, temperature, seismic, humidity, corrosion status, and ocean waves, so the possibility of catastrophe is high. Therefore, regular assessment is performed with data acquisition and transmission systems. The data are used to evaluate bridge condition. These measurement systems are called structural health monitoring (SHM) systems^[13-16]. Field tests are conducted using different sources of dynamic excitation, including ambient wind and ocean waves, traffic excitation, and impact excitation. A bridge's response under different dynamic excitation types is recorded using

accelerometers attached to the bridge deck. Data mining, which is drawing the attention of many scientists around the world, is adopted in this field in the form of vibration-based damage detection (VBDD) [17, 18, 19]. The basic idea of VBDD [20]. methods is that modal properties, including natural frequencies, mode shapes, and damping, are a function of physical properties of a structure, such as mass, stiffness, mechanical properties of materials, and boundary conditions. Therefore, changes in the physical properties of a structure will cause changes in the modal properties.

Therefore, this study suggests investigating the degradation in the overall stiffness (EJ_z) of structural span bridges [21, 22]. Characteristic parameters are selected on the basis of the power spectrum density, which is built from the acceleration signals of random vibrations on a bridge span's actual circulation. This new parameter can help monitor the degradation stiffness state of spans over time. It also evaluates different levels of defects and measuring points of the same span or of different spans in the same measuring time or in different times. This study also proposes changes in acreage in resonance regions of the power spectrum density concept; the process of monitoring and evaluating the degradation in the overall stiffness. These parameters are based on changes in the shape of change in acreage in the resonance regions of the power spectrum density during the operation process of the whole span's bridge. The goal is to evaluate the change in moment of the power spectrum density in different positions on the same span, or different spans on the same bridge.

2. Theory background

In this paper, the first five spectral moments are critically analyzed in the context of damage identification in a non-model-based approach to investigate their effectiveness and identify the most sensitive damage parameter or combination of parameters. These moments include the mean power (zero-order moment), mean-frequency (first-order moment), variance of the dataset (second-order moment), skewness (third-order moment), and data kurtosis (fourth-order moment). Subsequently, these spectral moments or a combination of moments that are the most sensitive and promising parameters for use in future structural damage identification studies are determined using model-based approaches and a Bayesian statistical framework. In general, for a given continuous zero-mean stationary Gaussian random process, the d^{th} -order non-central moments in the frequency domain and time domain, respectively, are given by the following:

$$\mu_f^d = \int_{-\infty}^{\infty} f^d \cdot S_{ww}(f) df \tag{1}$$

$$\mu_t^d = \int_{-\infty}^{\infty} t^d \cdot W^2(t) dt \tag{2}$$

Similarly, the central moments can be determined by subtracting the corresponding mean values at each frequency

and time as follows:

$$\mu_f^d = \frac{1}{\mu_f^0} \int_{-\infty}^{\infty} (f - \mu_f^1)^d \cdot S_{ww}(f) df \tag{3}$$

$$\mu_t^d = \frac{1}{\mu_t^0} \int_{-\infty}^{\infty} (t - \mu_t^1)^d \cdot W(t)^2 dt \tag{4}$$

Where μ_{df} and μ_{td} are d^{th} -order spectral moments in the frequency and time domains, respectively. $S_{ww}(f)$ is the response power spectral density or the vibrational energy distribution of a random process $W(t)$ in the frequency domain. $W(t)$ is the time series of interest; f is the signal frequency. For a discrete-time signal, the non-central and central spectral moments in the frequency domain can be defined as follows, respectively:

$$\mu_f^d = \frac{2}{N} \sum_{l=0}^{\frac{N}{2}-1} S(l) \cdot \left(\frac{l}{N \cdot \Delta t} \right)^d \tag{5}$$

$$\mu_t^d = \frac{2}{N \cdot \mu_f^0} \sum_{l=0}^{\frac{N}{2}-1} S(l) \cdot \left(\frac{l}{N \cdot \Delta t} - \mu_f^1 \right)^d \tag{6}$$

Where $2/N$ is the length of the one-sided power spectrum; $N = T/\Delta t$, where Δt is the sampling interval; and T is the signal observation time.

The different moments have various statistical interpretations and significance, which may provide useful information about the structural damage conditions. The level of significance should be viewed in the context of the degree of sensitivity and close relationships to the physical features of the structure. Therefore, the significance of each moment and its level of sensitivity to changes in the dynamic properties of the structure should be understood before these parameters are used in structural damage identification. In the following section, definitions of the spectral moments in the context of ordinary statistical terminology and their practical implications for structural damage identification are presented.

3. Results and discussion

The span of the Saigon Bridge, which contains prestressed concrete material, was surveyed during six rounds of measurement (over five years); the span's PSD is shown in Fig. 1. The power spectrum density (PSD) formed three resonance regions with significant amplitudes: from approximately 0 Hz to 8 Hz (first resonance region), from 8 Hz to 14 Hz (second region), and between 14 Hz and 24 Hz (third region). With a similar survey as that for prestressed concrete materials, another span on the Saigon Bridge with structural steel material was surveyed, as shown in Fig. 2. This figure shows that there were mainly two resonance regions with significant amplitudes: from around 0 Hz to 8 Hz (first resonance region) and between 8 Hz and 18 Hz (second region).

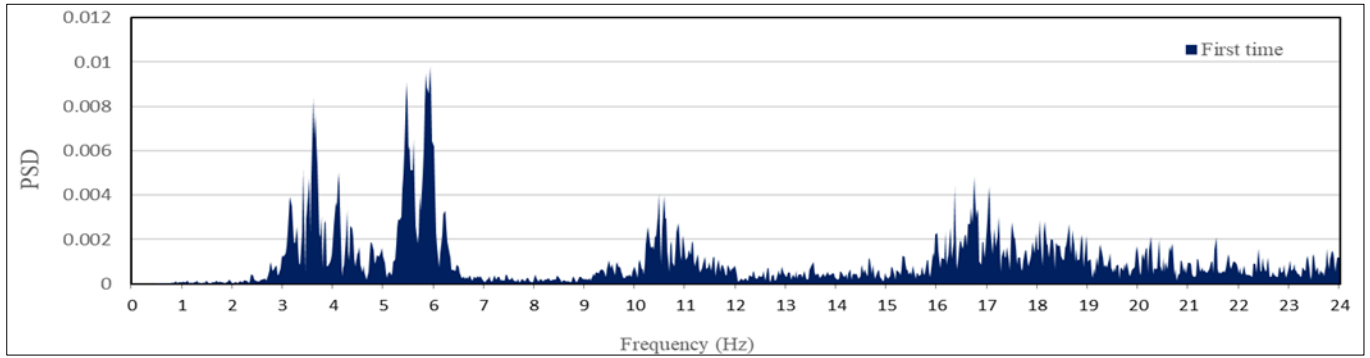


Fig 1: PSD of Saigon Bridge span with prestressed concrete material (first time)

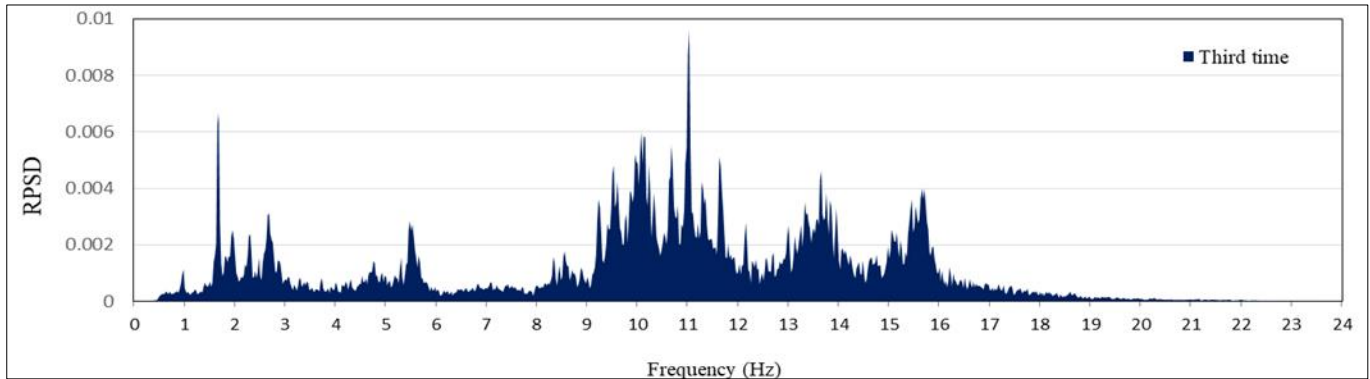
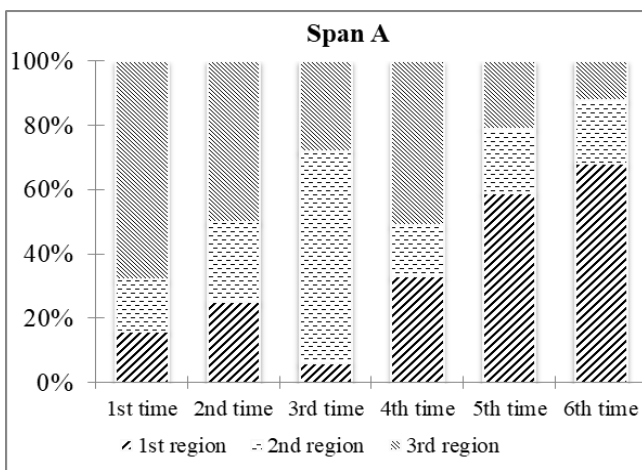


Fig 2: PSD of Saigon Bridge span with structural steel material (third time)

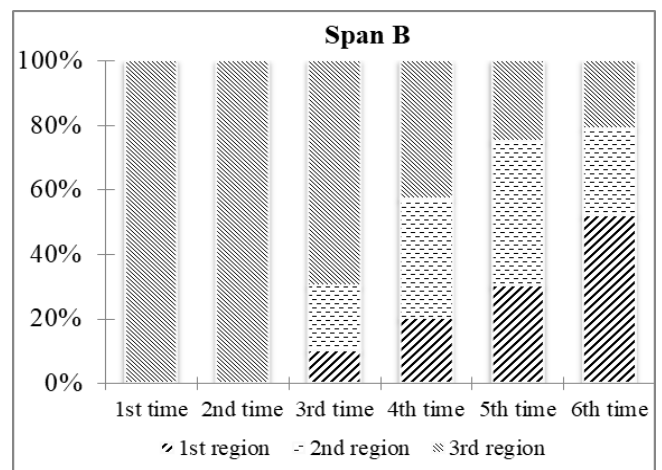
3.1. Characteristics’ change with the number of resonance regions of the actual PSD

In the PSD graphs coexisted in many resonance regions at the same measurement times. An actual vibration graph of data was generated at each measurement time. The Fourier analysis indicated that some PSDs involved only one resonance region; some PSDs included two resonance regions, and the others covered three resonance regions. Figs. 1 and 2 show that the total percentage of the PSD with the different structural materials (prestressed concrete and structural steel) on Saigon Bridge exhibited many changes

across the different measurement times. However, after over five years of health monitoring, the data of PSD with two or three resonance regions showed a significant downward trend, while the total PSD with only one resonance region experienced a dramatic upward trend. Thus, the operating time of the bridge clearly showed that the PSD’s probability to contain resonance regions at high frequencies will decline, and these PSDs will be replaced by those that have only one resonance region, although the traffic load remains unchanged.



(a)



(b)

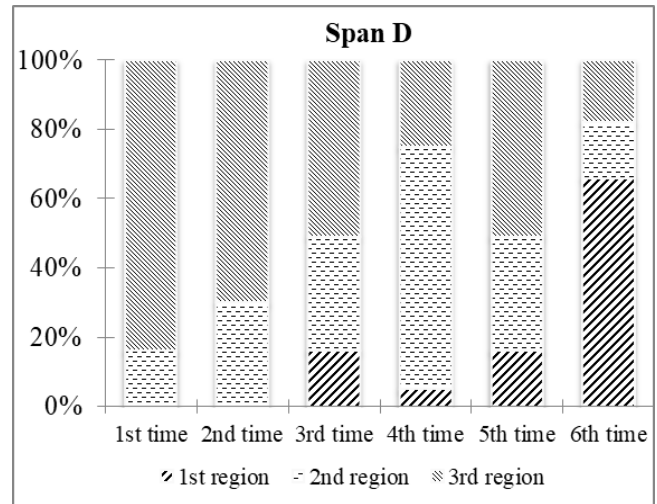
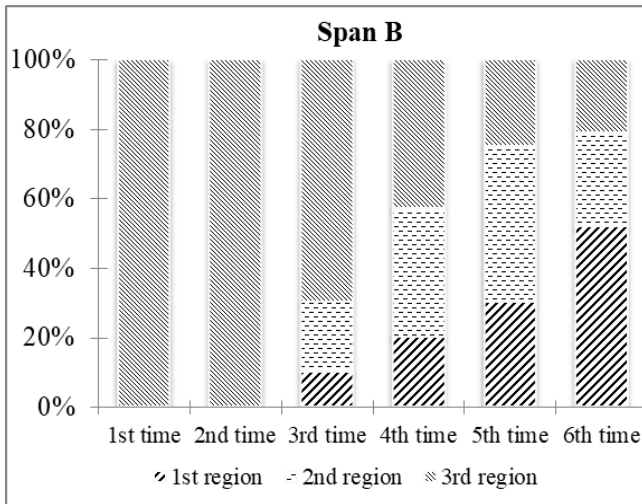


Fig 3: Percentage of total PSD with the same resonance region on prestressed concrete structure material

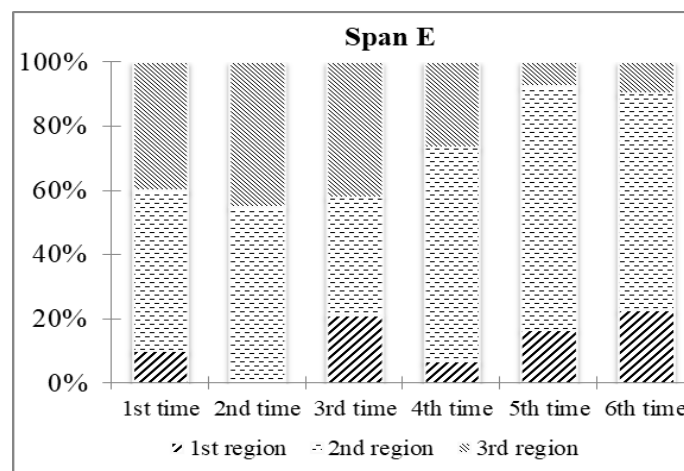


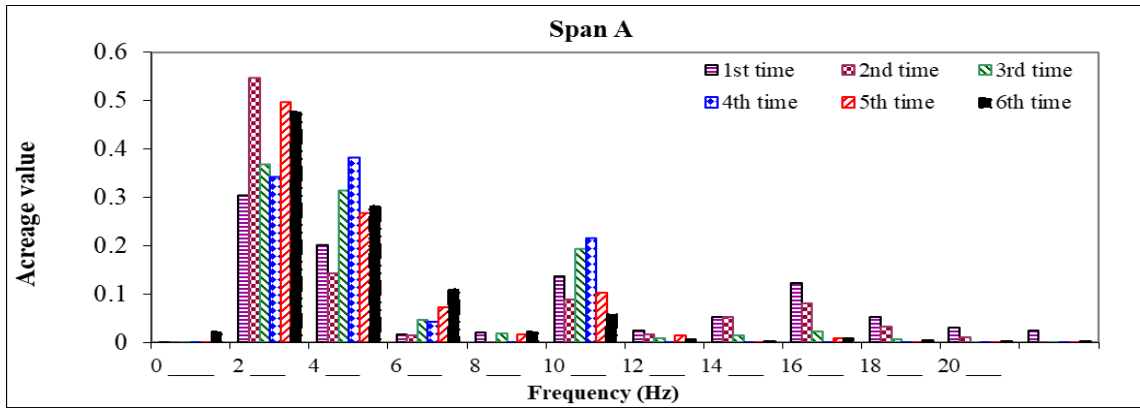
Fig 4: Percentage of total PSD with the same resonance region on steel structure material

The probability of appearance of PSDs with three resonance regions significantly decreased over the given period. According to mechanical theory, under the same source traffic load and throughout the operating time, a bridge’s span will weaken the bearing capacity; therefore, the amplitude of high-level harmonics will decrease accordingly. The theory also shows that the vibration power of the source traffic load will move from high-resonance regions to low-resonance ones. A comparison between the steel structure material and prestressed concrete material of the Saigon Bridge is shown in Figs. 3 and 4. The probability of appearance of the highest-resonance region of the prestressed concrete material structure changed more rapidly compared with that of the steel structure material in the same period. This finding is consistent with the structure material properties (the destruction time of steel material is longer than that of concrete). Hence, this paper offers a novel contribution by proposing an evaluation method of the bearing capacity and

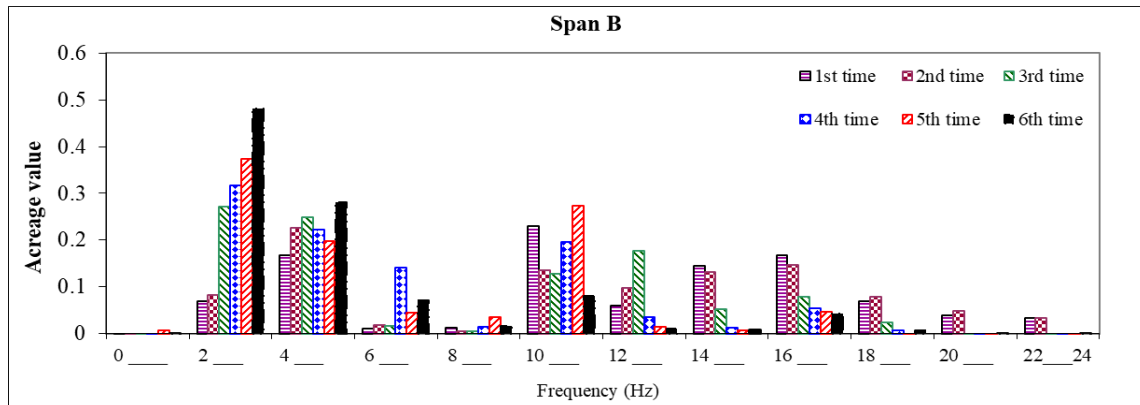
monitoring status of a bridge’s span during its operation.

3.2. Characteristics’ change of acreage in the resonance regions

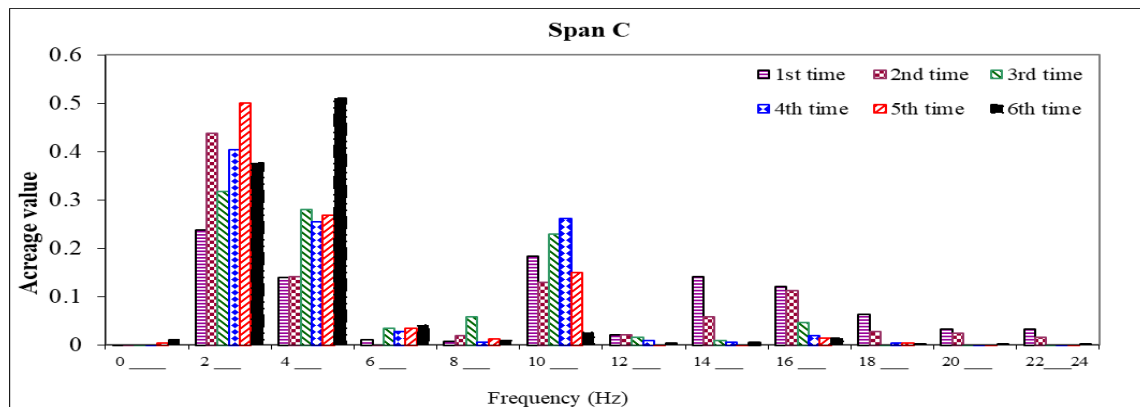
For a representation of the change in the shape of the resonance regions, special information is provided about the acreage value of the resonance regions in the PSD that were surveyed in a set data signal of the bridge’s span. The acreage values of the resonance regions in the PSD were limited by frequency ranges with a width of 2 Hz to understand the process of the acreage changes in each region. In terms of mechanics, the acreage value of a resonance region would represent the total vibration energy of the harmonics in the frequency range. With the frequency ranges equally divided into 2 Hz, the graphs in Figs. 5 and 6 show the acreage change of the resonance regions in some of the Saigon Bridge’s spans.



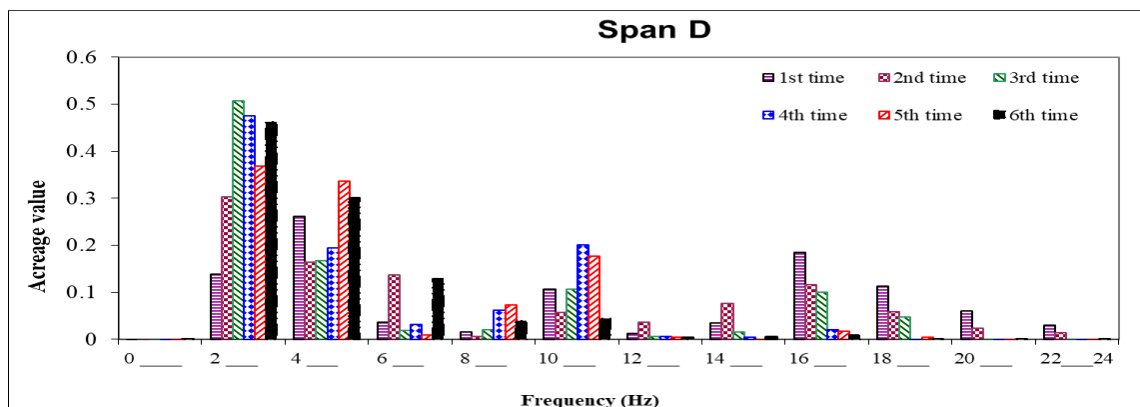
(a)



(b)



(c)



(d)

Fig 5: Acreage changes of PSD on the Saigon Bridge’s spans A, B, C, and D (prestressed concrete structure material)

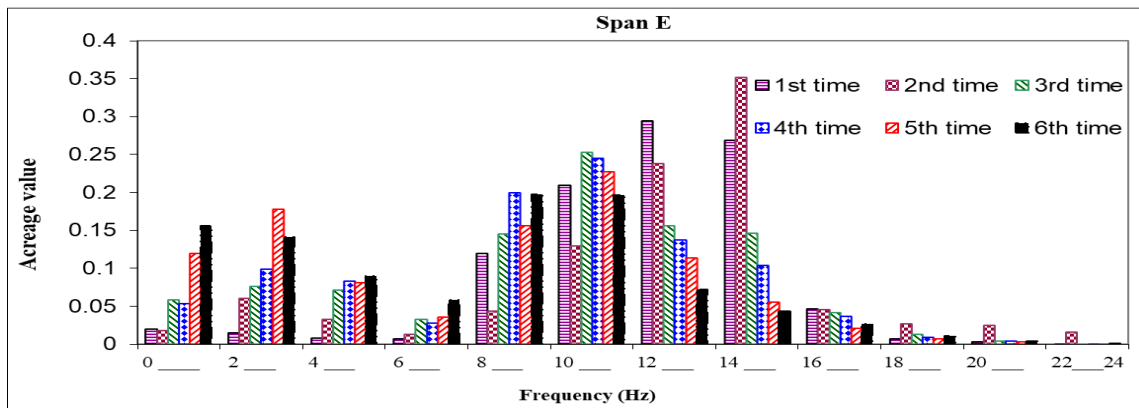


Fig 6: Acreage changes of PSD on the Saigon Bridge’s span E (prestressed concrete structure material)

A survey of the PSD share through the acreage values of the resonance regions revealed the following:

- All spans with prestressed concrete structure material on the Saigon Bridge exhibited the same characteristics when the acreage at the high frequencies (over 12 Hz) decreased over the given period. At the low frequencies (under 12 Hz). There was a seemingly unclear energy transition from the high-frequency regions to the low-frequency ones, and the amplitude harmonics significantly fluctuated.
- With the steel structure material of span E, the region acreage in the high-frequency ranges decreased continuously over time, as was the case with the concrete spans. However, the acreage in the other regions (low frequencies) exhibited a slight upward trend.

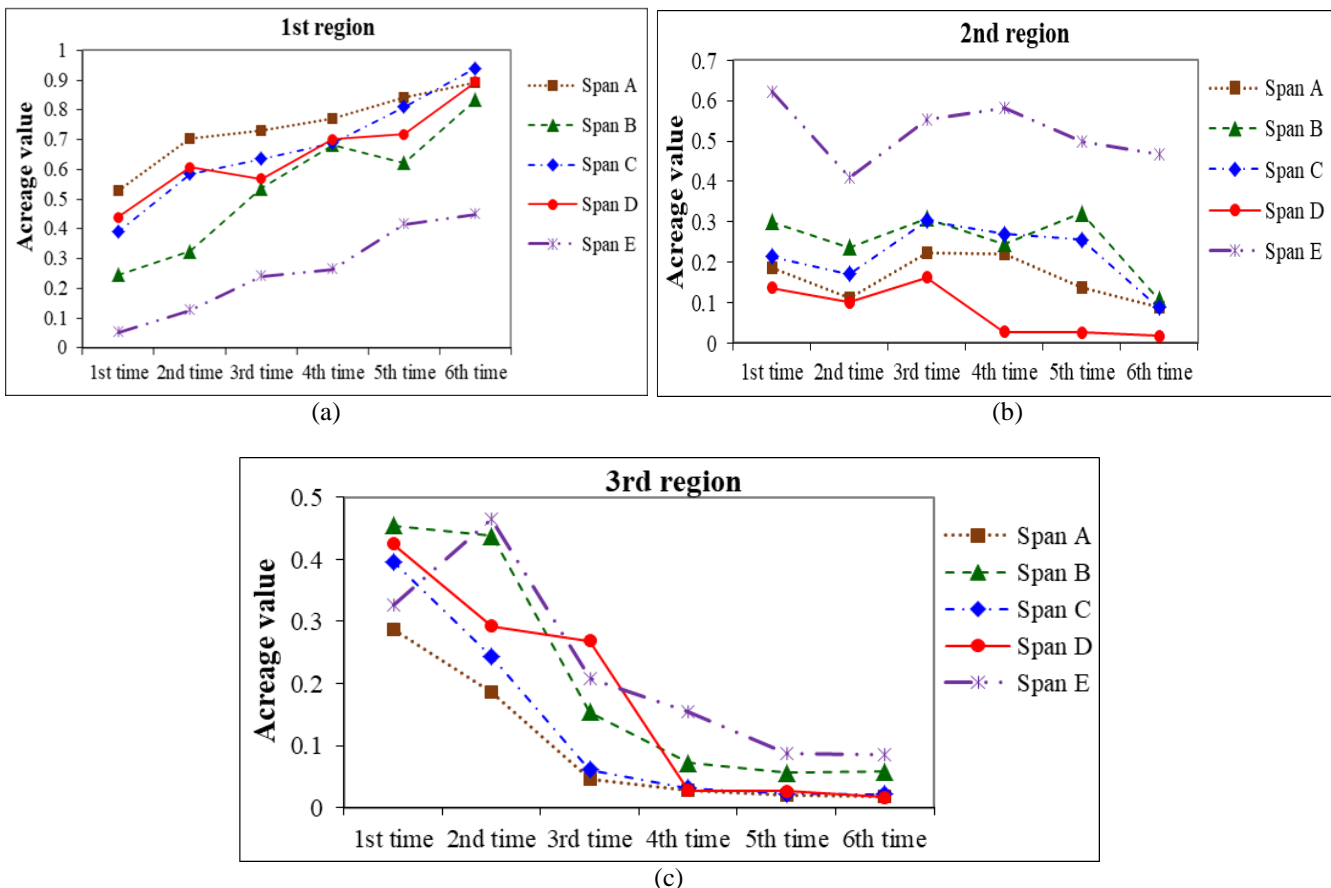


Fig 7: Acreage of PSD with the different resonance regions on some spans of the Saigon Bridge

In the high-frequency region (third region), the acreage value of the resonance regions experienced a downward trend over the given period. Over two measurement rounds (12/2011 and 2/2012) for all spans of the Saigon Bridge, the third region had significant energy proportions of around 40% and 30%, respectively, and reached the highest point of about 17

Hz. In the middle measurements (third round: 5/2012, fourth: 8/2012), the acreage value of the third resonance region dramatically declined to under 5%. This indicated an energy transmission from the third resonance region to the second or first resonance region. However, the acreage value in the second region did not show a co-variable increase over a

short time as like the first resonance region. From the fifth measurement (7/2015) to the sixth (10/2016), the acreage value of the second resonance region significantly decreased, while that of the first resonance region steeply increased. During the sixth measurement round, the amplitude spectrum of the area of the third resonance region in the PSD became very small or nonexistent. The main cause may be the transmission of the highest vibration energy from the high-frequency region to the low-frequency region; consequently, the energy became concentrated in the first resonance region. Thus, when the bearing capacity of the bridge's span decreased, the acreage value would determine the sensitivity with the operating status on the bridge on the basis of the highest- and lowest-frequency regions in the PSD graph.

4. Conclusions

The results of the present study showed the following:

- PSD coexisted with each other in many resonance regions at the same measurement times. An actual vibration graph of a set data was generated at each measurement time.
- The PSD's probability to contain resonant regions at high frequencies will decline, and such PSDs will be replaced by those that have only one resonance region, although the traffic load remains unchanged. The novel contribution of this study is an evaluation method of the bearing capacity and monitoring status of a bridge's span during its operation.

5. References

1. Shinae Jang, Hongki Jo, Soojin Cho, Kirill Mechitov, Jennifer A Rice, Sung-Han Sim et al. Structural health monitoring of a cable-stayed bridge using smart sensor technology: deployment and evaluation, *Smart Structures and Systems*. 2010; 6:5-6, 439-459.
2. Zaher. PhD thesis: An integrated vibration-based structural health monitoring system, Ottawa: Carleton University, Ottawa, 2002.
3. Wang S, Stratford T, Reynolds TPS. Linear creep of bonded FRP-strengthened metallic structures at warm service temperatures, *Construction and Building Materials*, vol. 283, pp. ID 122699, 2021.
4. Kai-Yuen Wong. Instrumentation and health monitoring of cable-supported bridges, *Structural Control and Health Monitoring*. 2004; 11(2):91-124.
5. Wang YW, Ni YQ, Zhang QH, Zhang C. Bayesian approaches for evaluating wind-resistant performance of long-span bridges using structural health monitoring data," *Structural Control and Health Monitoring*. 2021; 8:4.
6. Xiang Xu, Yon-Lin Xu, Yuan Ren, Qiao Huang. Site-Specific Extreme Load Estimation of a Long-Span Cable-Stayed Bridge," *Journal of Bridge Engineering*. 2021; 6:4. pp. ID 05021001, 2021.
7. American Association of State, Bridging the Gap: Restoring and Rebuilding the Nation's Bridges, American Association of State Highway and Transportation Officials, 2010.
8. Ko JM, Yiqing Ni, Wang JY, Sun ZG, Zhou XT. Studies of vibration-based damage detection of three cable-supported bridges in Hong Kong," in *International Conference on Engineering and Technological Sciences [ICET]*, The Hong Kong Polytechnic University Department of Civil and Environmental Engineering, 2000.
9. Ni YQ. Structural health monitoring of cable-supported bridges based on vibration measurements, in *Proceedings of the 9th International Conference on Structural Dynamics*, Eurodyn, 2014.
10. Qin Yang, Shaole Yu, Xuwei Zhang, Zhijun Wang, Junsheng Yan, Xinxi Chen. The Construction Technology of Roof Steel Structure in YanCheng NanYang Airport," *Advances in Civil Engineering*. 2018; 1:12, pp. ID 6386020.
11. Jungwee Lee, Kenneth Loh J, Hyun Sung Choi, Hohyun An. Effect of Structural Change on Temperature Behavior of a Long-Span Suspension Bridge Pylon," *International Journal of Steel Structures*. 2019; 19:2073-2089.
12. Huaping Ding, Qinghong Shen and Sidan Du, "Autonomous main-cable vibration monitoring using wireless smart sensors for large-scale three-pylon suspension bridges: A case study," *Journal of Low Frequency Noise, Vibration and Active Control*. 2020; 39(3):604-615.
13. Ren Li, Tianjin Mo, Jianxi Yang, Shixin Jiang, Tong Li, Yiming Liu. Ontologies-based Domain Knowledge Modeling and Heterogeneous Sensor Data Integration for Bridge Health Monitoring Systems, *IEEE Transactions on Industrial Informatics*. 2020; 1:1. pp. ID 2967561.
14. Ni YQ, Wang YW, Zhang C. A Bayesian approach for condition assessment and damage alarm of bridge expansion joints using long-term structural health monitoring data," *Engineering Structures*. 2020; 212 ID 110520.
15. Wang YW, Ni YQ. Bayesian dynamic forecasting of structural strain response using structural health monitoring data," *Structural Control and Health Monitoring*. 2020; 27:8, pp. ID 2575.
16. John Thedy, Kuo-Wei Liao, Chun-Chieh Tseng, Chia-Ming Liu. Bridge Health Monitoring via Displacement Reconstruction-Based NB-IoT Technology, *Applied Sciences*. 2020; 10:24, pp. ID 8878.
17. Thao Nguyen D, Thanh Nguyen Q, Tam Nhat N, Nguyen-Xuan H, Nhi Ngo K. A novel approach based on viscoelastic parameters for bridge health monitoring: A case study of Saigon bridge in Ho Chi Minh City – Vietnam," *Mechanical Systems and Signal Processing*. 2020, 141, pp. ID 106728.
18. Thanh Nguyen Q, Thao Nguyen D, Lam Tran Q, Nhi Ngo K. A New Insight to Vibration Characteristics of Spans under Random Moving Load: Case Study of 38 Bridges in Ho Chi Minh City, Vietnam," *Shock and Vibration*, 2020, pp. ID 1547568.
19. Nguyen Thi Giang. Free Vibration Exploration of Rotating FGM Porosity Beams under Axial Load considering the Initial Geometrical Imperfection," *Mathematical Problems in Engineering*. 2021, ID 5519946.
20. Bin Xu, Danhui Dan and Yiming Zhao. Frequency-Domain Estimation Method for Vibration-Induced Additional Cable Tension Based on Acceleration Monitoring, *Journal of Vibration and Acoustics*. 2019; 141:6, pp. ID 4044673, 2019.
21. Thanh Q, Nguyen and Hoang B. Nguyen, "Detecting and Evaluating Defects in Beams by Correlation Coefficients," *Shock and Vibration*, 2021, pp. ID 6536249.
22. Michal Venglár, Milan Sokol. Case study: The Harbor Bridge in Bratislava, *Structural Concrete*. 2020; 21(6):2736-2748.